

Low-energy magnetic excitations in the mixed spin- $(\frac{1}{2}, \frac{5}{2})$ chain

H. Yamaguchi^{1,*}, Y. Iwasaki,¹ Y. Kono,¹ T. Okita,¹ A. Matsuo,² M. Akaki³, M. Hagiwara,³ and Y. Hosokoshi¹

¹Department of Physical Science, Osaka Prefecture University, Osaka 599-8531, Japan

²Institute for Solid State Physics, the University of Tokyo, Chiba 277-8581, Japan

³Center for Advanced High Magnetic Field Science (AHMF), Graduate School of Science, Osaka University, Osaka 560-0043, Japan



(Received 8 June 2020; accepted 14 August 2020; published 28 August 2020)

We present studies on the low-energy magnetic excitations in the Lieb-Mattis (LM) ferrimagnetic phase. We investigate the low-energy magnetic excitations in the mixed spin- $(\frac{1}{2}, \frac{5}{2})$ chain (4-Br-*o*-MePy-V)FeCl₄ based on low-temperature specific heat and multifrequency electron spin resonance (ESR) measurements. A clear \sqrt{T} term is observed in the specific heat, which indicates a contribution of the low-energy magnetic excitation with a ferromagnetic quadratic dispersion expected in the LM ferrimagnetic state. Through the ESR mode analysis, we examine the effects of magnetic anisotropy on the excited states in the LM plateau phase.

DOI: [10.1103/PhysRevB.102.060408](https://doi.org/10.1103/PhysRevB.102.060408)

Variations of spin size in one-dimensional (1D) spin chains cause a variety of quantum many-body phenomena through strong quantum fluctuations, such as the Haldane state [1]. The topological ground state of the Haldane chain can be described by a valence-bond picture [2], where each integer spin is considered as a collection of $S = \frac{1}{2}$ spins and forms a singlet state between $S = \frac{1}{2}$ spins on the different sites. Mixed spin chains with antiferromagnetically coupled alternating $S = \frac{1}{2}$ and $S > \frac{1}{2}$ spins have also attracted considerable attention as quantum spin systems with topological properties [3–13]. According to the Lieb-Mattis (LM) theorem, the ground state of the mixed spin- $(\frac{1}{2}, S)$ Heisenberg chain is a ferrimagnet with a value of $S - \frac{1}{2}$ [14]. Furthermore, the topological argument by the Oshikawa-Yamanaka-Affleck criterion [15], which is confirmed to provide a necessary condition for a magnetization plateau [16–22], predicts the appearance of a quantized magnetization plateau at $(S - \frac{1}{2})/(S + \frac{1}{2})$. A unique feature of the LM ferrimagnet is the presence of gapless ferromagnetic and gapped antiferromagnetic (AF) spin-wave excitations. Because the gapless ferromagnetic excitation exhibits a quadratic dispersion relation in the long-wavelength limit, the low-temperature specific heat is expected to show a square root temperature dependence. In real compounds, although there are some contributions from other dispersions associated with finite interchain couplings, a large square root contribution is expected to appear in the low-temperature region of the specific heat. Several mixed spin- $(\frac{1}{2}, S)$ Heisenberg chains had been experimentally investigated more than 20 years ago. Several bimetallic coordination compounds [23–28] and molecular materials composed of organic radicals and metals [29,30] have been reported to form mixed spin chains. Some of these compounds show a tendency towards a magnetization plateau, but this behavior does not provide sufficient evidence of the LM plateau in terms of the energy gap [23,25,28].

Recently, we reported the observation of a LM plateau in a mixed spin- $(\frac{1}{2}, \frac{5}{2})$ chain formed by the verdazyl-based salt (4-Br-*o*-MePy-V)FeCl₄ [4-Br-*o*-MePy-V=3-(5-Br-1-methylpyridinium-2-yl)-1,5-diphenylverdazyl] [31]. Verdazyl radicals are among the group of stable organic radicals and have a delocalized spin- $\frac{1}{2}$ expanded over a molecule [32]. In this compound, the verdazyl radical 4-Br-*o*-MePy-V and the FeCl₄ anion have spin- $\frac{1}{2}$ and $\frac{5}{2}$, respectively, and the exchange interactions between those spins form a mixed spin- $(\frac{1}{2}, \frac{5}{2})$ chain with a slight bond alternation ($0.7 < J'/J < 1$), as shown in Fig. 1. The observed magnetization curve exhibits a clear $\frac{2}{3}$ LM plateau between approximately 2 and 30 T and a subsequent quantum phase transition towards the gapless Luttinger-liquid phase. We explained the observed magnetic behavior quantitatively in terms of the mixed spin- $(\frac{1}{2}, \frac{5}{2})$ chain with $J/k_B \approx 9$ –11 K, which is defined in the Heisenberg spin Hamiltonian given by $\mathcal{H} = J \sum_i s_{2i-1} \cdot S_{2i} + J' \sum_i S_{2i} \cdot s_{2i+1}$, where s and S are the spin- $\frac{1}{2}$ and $-\frac{5}{2}$ operators, respectively. Because the LM theorem is applied even in the case of the alternating type, the ground state is expected to become a ferrimagnetic state with $S_{\text{tot}}^z = 2$. We can understand this by the valence bond picture schematically illustrated in Fig. 1, where the two spin- $\frac{1}{2}$ particles on the different sites form a nonmagnetic singlet dimer through J . In the low-field region of (4-Br-*o*-MePy-V)FeCl₄, a phase transition to an AF ordered state appears owing to the weak but finite interchain couplings.

In this Rapid Communication, we report the results of the low-temperature specific heat and ESR measurements on the mixed spin- $(\frac{1}{2}, \frac{5}{2})$ chain (4-Br-*o*-MePy-V)FeCl₄. We observe a clear \sqrt{T} term in the low-temperature region of the specific heat, which indicates a contribution of the low-energy magnetic excitation with the ferromagnetic quadratic dispersion expected in the LM ferrimagnetic state. Through an ESR mode analysis, we evaluate interchain AF interactions causing the ordered state of the $S_{\text{tot}} = 2$ spins and on-site biaxial anisotropy associated with the spin-flop transition. Furthermore, we examine the effects of the magnetic anisotropy

*Corresponding author: yamaguchi@p.s.osakafu-u.ac.jp

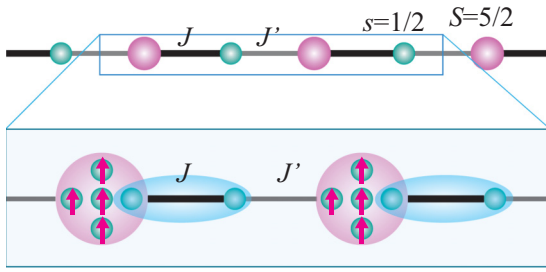


FIG. 1. Mixed spin- $(\frac{1}{2}, \frac{5}{2})$ chain composed of $s = \frac{1}{2}$ on the radical and $S = \frac{5}{2}$ on the FeCl_4 anion through J and J' ($J > J'$). The enlarged illustration shows the valence bond picture of the Lieb-Mattis ferrimagnetic state. The $S = \frac{5}{2}$ spins are composed of five $s = \frac{1}{2}$ spins, and the valence bond singlet pairs are formed by two $s = \frac{1}{2}$ spins.

on the low-energy excitation in the LM plateau phase and evaluate the anisotropic parameters.

Small single crystals of $(4\text{-Br-}o\text{-MePy-V})\text{FeCl}_4$ was prepared as described in our previous report [31]. The crystallographic parameters are as follows: monoclinic, space group $P2_1/c$, $a = 7.676(7)$ Å, $b = 19.425(15)$ Å, $c = 16.028(13)$ Å, $\beta = 94.962(16)^\circ$, $V = 2381(3)$ Å³, and $Z = 4$. The mixed spin chain composed of 4-Br-*o*-MePy-V with spin- $\frac{1}{2}$ and FeCl_4 with spin- $\frac{5}{2}$ are formed along the c axis. The specific heat was measured using a commercial calorimeter (PPMS, Quantum Design) by using a thermal relaxation method down to approximately 0.4 K. The ESR measurements were performed utilizing a vector network analyzer (ABmm), a superconducting magnet (Oxford Instruments) at AHMF in Osaka University. At frequencies between 10.8 and 34.1 GHz, we used laboratory-built cylindrical cavities. All experiments were performed using small randomly oriented single crystals.

As shown in Fig. 2(a), the specific heat C_p at zero field clearly exhibits a λ -type sharp peak associated with the phase transition to the AF order at $T_N = 4.8$ K. In magnetic fields, the phase transition temperature decreases with increasing fields and almost disappears above 2 T [31], which is consistent with the formation of the plateau phase with a spin gap. Figure 2(b) shows the field-temperature phase diagram associated with the ordered state obtained in our previous experimental study [31]. Although the lattice contributions are not subtracted from C_p , the magnetic contributions are expected to be dominant in the present low-temperature regions, as observed in other verdazyl-based compounds [33–37]. From Fig. 2(a), we can clearly observe a \sqrt{T} behavior in the low-temperature region of C_p/T . Considering the contributions of the low-energy excitations to the specific heat, this $T^{3/2}$ behavior of C_p indicates the existence of both 1D gapless quadratic ferromagnetic and linear AF magnon dispersions. Therefore, the long-wavelength spin excitations are described by the following dispersion relation: $\omega = v_x k_x^2 + v_y k_y$, where v_x and v_y are the spin wave dispersion coefficients for the ferromagnetic and AF excitations, respectively. The gapless quadratic ferromagnetic dispersion causing the \sqrt{T} contribution is exactly the low-lying magnon excitation expected in the LM ferrimagnetic state. The additional T -linear contribution from the AF magnon dispersion is considered to originate

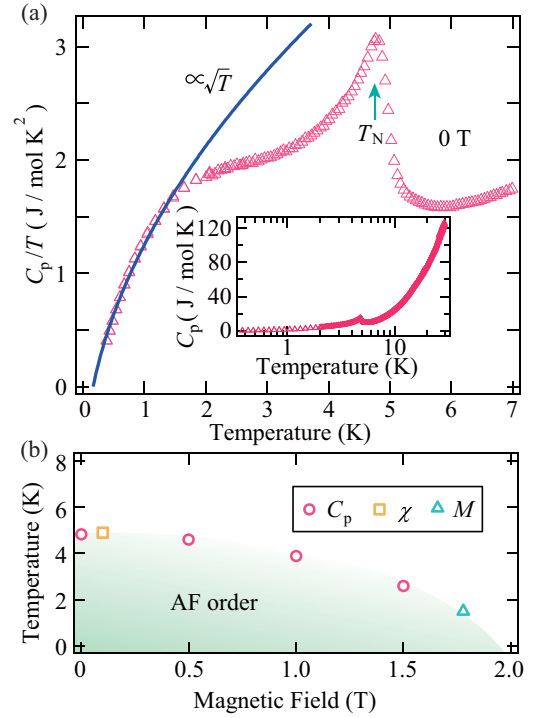


FIG. 2. (a) Low-temperature part of the specific heat of $(4\text{-Br-}o\text{-MePy-V})\text{FeCl}_4$ at zero field. The solid line indicates the \sqrt{T} behavior. The inset shows the specific heat up to 30 K. (b) Magnetic field vs temperature phase diagram showing the phase boundary for the second-order phase transition between the AF order and paramagnetic state. The spin-flop transition corresponds to a first-order transition within the AF order. The circles, square, and triangle indicate the phase boundaries determined from the specific heat C_p , magnetic susceptibility χ , and magnetization curve M , respectively [31].

from the dominant couplings between the mixed spin chains, yielding the AF order. As discussed in the theoretical studies [7,10], the LM ferrimagnetic state is expected to exhibit double peaks in the specific heat. The peak temperatures are expected to be approximately 3 and 15 K for the present model. In the experimental result, the interchain contribution below T_N and large lattice contributions above 10 K are considered to mask the clear peak structure.

Figure 3 shows the magnetization curve in the low-field region below T_N . The field-independent behavior above approximately 2 T corresponds to the LM plateau with $\frac{2}{3}$ magnetization, which continues up to approximately 30 T and increases again toward the saturation at approximately 40 T [31]. The field derivative of the magnetization curve (dM/dH) exhibits a distinct peak at approximately $H_{sf} = 0.48$ T, as shown in the inset of Fig. 3. This indicates a spin-flop transition caused by a small magnetic anisotropy, which we will discuss in the following ESR analysis. The magnetic moment of approximately $4\mu_B/\text{f.u.}$ at the LM plateau phase corresponds to the fully polarized $S_{\text{tot}} = 2$ spins along the field direction. This characteristic demonstrates that the low-field phase is an AF order of the $S_{\text{tot}} = 2$ spins. We evaluated the phase transition field to the LM plateau phase, H_{fp} , from the midpoint of the drastic change in dM/dH .

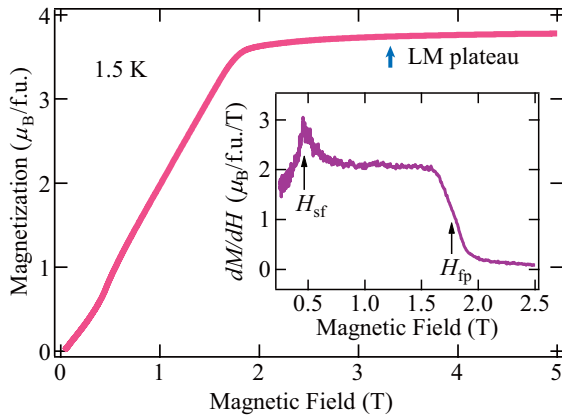


FIG. 3. Low-field magnetization curve of (4-Br-*o*-MePy-V)FeCl₄ at 1.5 K [31]. The field-independent behavior above approximately 2 T corresponds to the Lieb-Mattis plateau, which is identical to the fully polarized $S_{\text{tot}} = 2$ spins along the field direction. The inset shows the field derivative of the magnetization curve (dM/dH). H_{sf} and H_{fp} indicate the spin-flop transition and transition to the fully polarized state, respectively.

We performed ESR measurements to evaluate the magnetic anisotropy in the present spin system. Because our experiments were performed using small, randomly oriented single crystals, the resonance fields for the principal axes are observed as minimum and inflection points. Figure 4(a) shows the temperature dependence of the absorption spectra at 82.8 GHz. In the high-temperature regions, the observed signals are considered as the paramagnetic resonance. With decreasing temperature, the resonance spectra dramatically broaden in the vicinity of T_N . This behavior indicates that the appearance of the magnetic anisotropy is accompanied by the phase transition. The magnetic anisotropy of the organic radical and high spin $3d^5$ is known to be quite small and almost isotropic at experimental temperatures. Thus, the observed anisotropy is considered to originate mainly from an anisotropic field arising from dipole-dipole interactions. Figures 4(b) and 4(c) show the frequency dependencies of

the resonance fields at 1.8 K. As shown in Fig. 4(b), at low frequencies, the resonance signals exhibit a broad character, and the resonance fields show discontinuous frequency dependence. As shown in Fig. 4(c), at high frequencies, the resonance fields are almost proportional to the frequency. Figure 5 shows frequency-field diagrams of all the resonance fields. Because a zero-field gap of ~ 20 GHz corresponds to the energy scale of H_{sf} , those resonance fields suggest conventional AF resonance modes in an anisotropic two-sublattice model [38–42].

Taking the experimental conditions for $T < T_N$ and $H < H_{\text{fp}}$, we analyzed the experimental results in terms of a mean-field approximation assuming $S = 2$ ferromagnetic chains coupled by AF interaction J_{inter} . We also considered on-site biaxial anisotropy causing the spin-flop transition at H_{sf} . Because the $S = 2$ spins in each chain are arranged along the same direction, the effective intrachain ferromagnetic interactions do not affect the resonance conditions. Thus, we consider only the interchain AF interaction, and the spin Hamiltonian is expressed as

$$\mathcal{H} = nJ_{\text{inter}} \sum_{\langle i,j \rangle} \mathbf{S}_i \cdot \mathbf{S}_j + D \sum_i (S_i^z)^2 + E \sum_i \{ (S_i^x)^2 - (S_i^y)^2 \} - g\mu_B \sum_i \mathbf{S}_i \cdot \mathbf{H}, \quad (1)$$

where $\langle i, j \rangle$ denotes the neighboring spin pairs between two chains, n is the number of nearest-neighbor chains, D and E are on-site anisotropies ($D, E < 0$), and \mathbf{S} is an $S = 2$ classical spin. The spin structure is described by a two-sublattice model, and we derive the resonance conditions by solving the equation of motion for the sublattice moments [43,44]. The spin configurations are also required to obtain the resonance conditions. The spins are aligned along the easy axis (z axis) under zero-field conditions. For $H \parallel z$, the discontinuous spin-flop transition occurs at H_{sf} . The value of H_{sf} is expressed as $4\sqrt{(-D + E)(D - E + nJ_{\text{inter}})}/g\mu_B$, which corresponds to the lowest zero-field energy gap of resonance modes. Above H_{sf} , the two sublattices are tilted with respect to the field direction with equivalent angles. For the other principal axes,

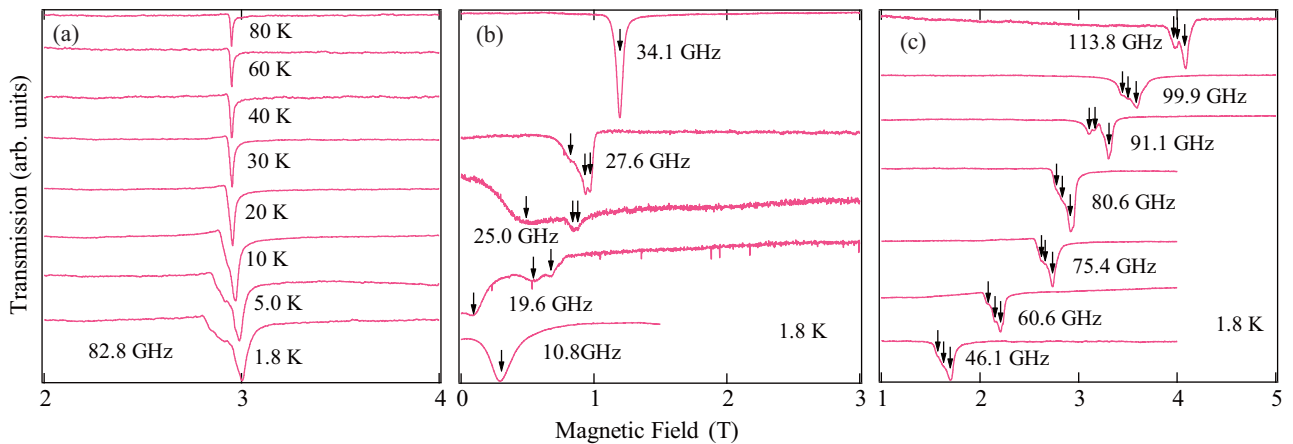


FIG. 4. (a) Temperature dependence of ESR absorption spectra of (4-Br-*o*-MePy-V)FeCl₄ at 82.8 GHz. Frequency dependence of ESR absorption spectra at 1.8 K for (b) low frequencies measured by cylindrical cavities and (c) directly detected high frequencies. The arrows indicate resonance signals.

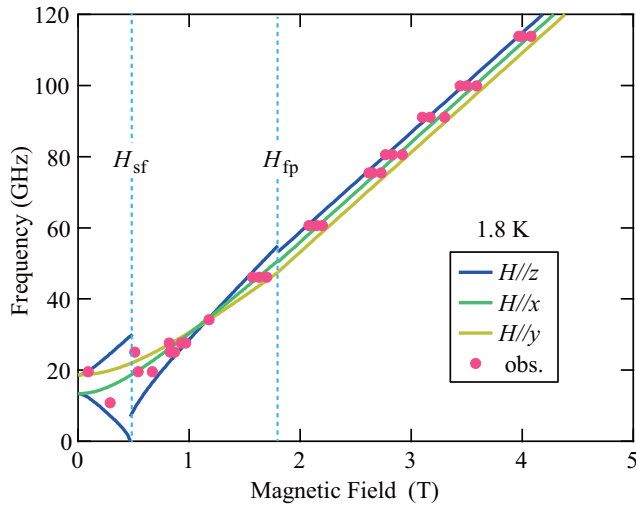


FIG. 5. Frequency-field plot of the ESR fields at 1.8 K. The solid lines indicate the calculated resonance modes for the principal axes. The discontinuous changes in the lines correspond to the spin-flop transition at H_{sf} and transition to the fully polarized state of $S_{tot} = 2$ at H_{fp} .

where the external fields are applied perpendicular to the easy axis, the two sublattices are tilted from the easy axis with equivalent angles along each field direction. Then, the angles between the sublattice moment and the external field for both directions can be determined by minimizing the free energy. At H_{fp} , the sublattice moments are fully polarized along the field direction. We determined the parameters considering the values of H_{sf} and H_{fp} . As shown in Fig. 5, we obtain a good fit between the experimental and calculated results with the following parameters: $nJ_{inter}/k_B = 0.64$ K, $D/k_B = -0.055$ K, and $E/k_B = -0.019$ K. The calculated results demonstrate typical AF resonance modes with biaxial anisotropy in a two-sublattice model. The energy scale of the on-site anisotropy is the same as those of other veradzyl-based salts with $FeCl_4$ anions [41,42]; thus, the small magnetic anisotropy in this compound is also considered to originate from a magnetic dipole-dipole interaction.

Here, we consider the resonance modes in the LM plateau phase above H_{fp} . The ESR measurements provide information on the long-wavelength limit of magnon excitations on the LM ferrimagnetic state; thus, the resonance fields are expected to reflect the magnetic anisotropy of the excitations at $k = 0$. In the present alternate model with $\alpha < 1$, the ground state can be described by using $|S_{tot}, S_{tot}^z\rangle$. The first-order perturbation

treatment of J' and on-site anisotropy indicates that the ground state can be regarded as $\prod_j |2, +2\rangle_j$. Therefore, a single $S_{tot} = 2$ spin with on-site biaxial anisotropy is an effective model to evaluate the effects of the magnetic anisotropy on the magnon dispersions. The spin Hamiltonian is expressed as

$$\mathcal{H} = D(S_{tot}^z)^2 + E\{(S_{tot}^x)^2 - (S_{tot}^y)^2\} - g\mu_B S_{tot} \cdot \mathbf{H}. \quad (2)$$

Considering the low experimental temperature, only the transitions from the ground state are observed. In such case, the ESR selection rule permits one resonance mode for each field direction. We obtain a good agreement between the experimental and calculated results with $D/k_B = -0.045$ and $E/k_B = -0.015$ K, which are indeed very close to those evaluated from the above analysis in the ordered phase. The corresponding transitions between the $S = 2$ states can be identified in our previous numerical study in Ref. [45].

In summary, we performed low-temperature specific heat C_p and ESR measurements on the mixed spin- $(\frac{1}{2}, \frac{5}{2})$ chain (4-Br-*o*-MePy-V)FeCl₄. The specific heat in the low-temperature region exhibited almost $T^{3/2}$ dependence, which indicates a \sqrt{T} and T -linear terms originating from the 1D gapless quadratic ferromagnetic and linear AF dispersions, respectively. The existence of the ferromagnetic dispersion causing the \sqrt{T} contribution demonstrates the gapless magnon excitation expected in the LM ferrimagnetic state. Through the ESR resonance mode analysis, we evaluated the interchain AF interactions causing the ordered state of the $S = 2$ total spins and on-site biaxial anisotropy associated with the spin-flop transition. Furthermore, we examined the effects of magnetic anisotropy on the low-energy magnon excitations in the LM plateau phase. These results provide definitive insights into the low-energy magnon excitations in the mixed spin- $(\frac{1}{2}, \frac{5}{2})$ chains forming the LM ferrimagnetic state and will stimulate further studies on the topological properties of various mixed spin chains.

We thank T. Tonegawa, K. Okamoto, and S. C. Furuya for valuable discussions. This research was partly supported by Grant for Basic Science Research Projects from KAKENHI (Grants No. 17H04850, No. 19J01004, and No. 19H04550), the Shorai Foundation for Science and Technology, Izumi Science and Technology Foundation, SEI Group CSR Foundation, and Nanotechnology Platform Program (Molecule and Material Synthesis) of the Ministry of Education, Culture, Sports, Science and Technology (MEXT), Japan. A part of this work was performed at the Center for Advanced High Magnetic Field Science in Osaka University under the interuniversity cooperative research program of the joint-research program of ISSP, the University of Tokyo.

- [1] F. D. M. Haldane, *Phys. Rev. Lett.* **50**, 1153 (1983).
- [2] I. Affleck, T. Kennedy, E. H. Lieb, and H. Tasaki, *Phys. Rev. Lett.* **59**, 799 (1987).
- [3] S. Brehmer, H.-J. Mikeska, and S. Yamamoto, *J. Phys.: Condens. Matter* **9**, 3921 (1997).

- [4] S. K. Pati, S. Ramasesha, and D. Sen, *Phys. Rev. B* **55**, 8894 (1997).
- [5] S. K. Pati, S. Ramasesha, and D. Sen, *J. Phys.: Condens. Matter* **9**, 8707 (1997).
- [6] J. Strečka, *Acta Phys. Pol., A* **131**, 624 (2017).

- [7] A. S. F. Tenório, R. R. Montenegro-Filho, and M. D. Coutinho-Filho, *J. Phys.: Condens Matter* **23**, 506003 (2011).
- [8] K. Maisinger, U. Schollwöck, S. Brehmer, H. J. Mikeska, and S. Yamamoto, *Phys. Rev. B* **58**, R5908(R) (1998).
- [9] S. Yamamoto and T. Fukui, *Phys. Rev. B* **57**, R14008(R) (1998).
- [10] T. Nakanishi and S. Yamamoto, *Phys. Rev. B* **65**, 214418 (2002).
- [11] W. M. da Silva and R. R. Montenegro-Filho, *Phys. Rev. B* **96**, 214419 (2017).
- [12] W. M. da Silva and R. R. Montenegro-Filho, *J. Low Temp. Phys.* **187**, 712 (2017).
- [13] L. M. Verfssimo, M. S. S. Pereira, J. Strečka, and M. L. Lyra, *Phys. Rev. B* **99**, 134408 (2019).
- [14] E. Lieb and D. Mattis, *J. Math. Phys.* **3**, 749 (1962).
- [15] M. Oshikawa, M. Yamanaka, and I. Affleck, *Phys. Rev. Lett.* **78**, 1984 (1997).
- [16] Y. Narumi, K. Kindo, M. Hagiwara, H. Nakano, A. Kawaguchi, K. Okunishi, and M. Kohno, *Phys. Rev. B* **69**, 174405 (2004).
- [17] H. Kikuchi, Y. Fujii, M. Chiba, S. Mitsudo, T. Idehara, T. Tonegawa, K. Okamoto, T. Sakai, T. Kuwai, and H. Ohta, *Phys. Rev. Lett.* **94**, 227201 (2005).
- [18] Z. W. Ouyang, Y. C. Sun, J. F. Wang, X. Y. Yue, R. Chen, Z. X. Wang, Z. Z. He, Z. C. Xia, Y. Liu, and G. H. Rao, *Phys. Rev. B* **97**, 144406 (2018).
- [19] T. Susuki, N. Kurita, T. Tanaka, H. Nojiri, A. Matsuo, K. Kindo, and H. Tanaka, *Phys. Rev. Lett.* **110**, 267201 (2013).
- [20] A. N. Vasiliev, O. S. Volkova, E. A. Zvereva, E. A. Ovchenkov, I. Munaò, L. Clark, P. Lightfoot, E. L. Vavilova, S. Kamusella, H.-H. Klauss, J. Werner, C. Koo, R. Klingeler, and A. A. Tsirlin, *Phys. Rev. B* **93**, 134401 (2016).
- [21] Y. H. Matsuda, N. Abe, S. Takeyama, H. Kageyama, P. Corboz, A. Honecker, S. R. Manmana, G. R. Foltin, K. P. Schmidt, and F. Mila, *Phys. Rev. Lett.* **111**, 137204 (2013).
- [22] H. Yamaguchi, T. Okubo, S. Kittaka, T. Sakakibara, K. Araki, K. Iwase, N. Amaya, T. Ono, and Y. Hosokoshi, *Sci. Rep.* **5**, 15327 (2015).
- [23] M. Verdaguer, A. Gleizes, J. P. Renard, and J. Seiden, *Phys. Rev. B* **29**, 5144 (1984).
- [24] A. Gleizes and M. Verdaguer, *J. Am. Chem. Soc.* **103**, 7373 (1981).
- [25] O. Kahn, Y. Pei, M. Verdaguer, J. P. Renard, and J. Sletten, *J. Am. Chem. Soc.* **110**, 782 (1988).
- [26] P. J. Van Koningsbruggen, O. Kahn, K. Nakatani, Y. Pei, J. P. Renard, M. Drillon, and P. Legoll, *Inorg. Chem.* **29**, 3325 (1990).
- [27] M. Hagiwara, K. Minami, Y. Narumi, K. Tatani, and K. Kindo, *J. Phys. Soc. Jpn.* **67**, 2209 (1998).
- [28] M. Hagiwara, Y. Narumi, K. Minami, K. Tatani, and K. Kindo, *J. Phys. Soc. Jpn.* **68**, 2214 (1999).
- [29] A. Caneschi, D. Gatteschi, and R. Sessoli, *Inorg. Chem.* **32**, 4612 (1993).
- [30] K. Fegy, D. Luneau, E. Belorizky, M. Novac, J.-L. Tholence, C. Paulsen, T. Ohm, and P. Rey, *Inorg. Chem.* **37**, 4524 (1998).
- [31] H. Yamaguchi, T. Okita, Y. Iwasaki, Y. Kono, N. Uemoto, Y. Hosokoshi, T. Kida, T. Kawakami, A. Matsuo, and M. Hagiwara, *Sci. Rep.* **10**, 9193 (2020).
- [32] B. D. Koivisto and R. G. Hicks, *Coord. Chem. Rev.* **249**, 2612 (2005).
- [33] K. Iwase, H. Yamaguchi, T. Ono, Y. Hosokoshi, T. Shimokawa, Y. Kono, S. Kittaka, T. Sakakibara, A. Matsuo, and K. Kindo, *Phys. Rev. B* **88**, 184431 (2013).
- [34] H. Yamaguchi, T. Okubo, K. Iwase, T. Ono, Y. Kono, S. Kittaka, T. Sakakibara, A. Matsuo, K. Kindo, and Y. Hosokoshi, *Phys. Rev. B* **88**, 174410 (2013).
- [35] H. Yamaguchi, Y. Shinpuku, T. Shimokawa, K. Iwase, T. Ono, Y. Kono, S. Kittaka, T. Sakakibara, and Y. Hosokoshi, *Phys. Rev. B* **91**, 085117 (2015).
- [36] H. Yamaguchi, H. Miyagai, M. Yoshida, M. Takigawa, K. Iwase, T. Ono, N. Kase, K. Araki, S. Kittaka, T. Sakakibara, T. Shimokawa, T. Okubo, K. Okunishi, A. Matsuo, and Y. Hosokoshi, *Phys. Rev. B* **89**, 220402(R) (2014).
- [37] H. Yamaguchi, Y. Tamekuni, Y. Iwasaki, R. Otsuka, Y. Hosokoshi, T. Kida, and M. Hagiwara, *Phys. Rev. B* **95**, 235135 (2017).
- [38] C. Kittel, *Phys. Rev.* **82**, 565 (1951).
- [39] M. Hagiwara, K. Katsumata, I. Yamada, and H. Suzuki, *J. Phys.: Condens. Matter.* **8**, 7349 (1996).
- [40] R. S. Fishman, S.-i. Shinozaki, A. Okutani, D. Yoshizawa, T. Kida, M. Hagiwara, and M. W. Meisel, *Phys. Rev. B* **94**, 104435 (2016).
- [41] Y. Iwasaki, T. Kida, M. Hagiwara, T. Kawakami, Y. Hosokoshi, Y. Tamekuni, and H. Yamaguchi, *Phys. Rev. B* **97**, 085113 (2018).
- [42] Y. Iwasaki, T. Kida, M. Hagiwara, T. Kawakami, Y. Kono, S. Kittaka, T. Sakakibara, Y. Hosokoshi, and H. Yamaguchi, *Phys. Rev. B* **98**, 224411 (2018).
- [43] H. Tanaka, Y. Kaahwa, T. Hasegawa, M. Igarashi, S. Teraoka, K. Iio, and K. Nagata, *J. Phys. Soc. Jpn.* **58**, 2930 (1989).
- [44] H. Yamaguchi, S. Kimura, M. Hagiwara, Y. Nambu, S. Nakatsuji, Y. Maeno, A. Matsuo, and K. Kindo, *J. Phys. Soc. Jpn.* **79**, 054710 (2010).
- [45] H. Yamaguchi, Y. Shinpuku, Y. Kono, S. Kittaka, T. Sakakibara, M. Hagiwara, T. Kawakami, K. Iwase, T. Ono, and Y. Hosokoshi, *Phys. Rev. B* **93**, 115145 (2016).